PCCP

Accepted Manuscript

ROYAL SOCIETY OF CHEMISTRY

www.rsc.org/pccp

Chemical Science

ARTICLE

Received 00th January 20xx,
Accepted 00th January 20xx

DOI: 10.1039/x0xx00000x

www.rsc.org/

Confined water in imidazolium based ionic liquids: a supramolecular guest@host complex case

Marcileia Zanatta, [a] Anne-Lise Girard, [a] Graciane Marin, [a] Gunter Ebeling, [a] Francisco P. dosSantos, [a] Chiara Valsecchi, [a] Hubert Stassen, [a] Paolo R. Livotto, [a] William Lewis[b] and Jairton Dupont*[, a, b]

It is well known that the macroscopic physico-chemical properties of ionic liquids (ILs) are influenced by the presence of water that strongly interferes on the supramolecular organization of these fluids. However, little is known about the function of water traces *within this confined space and restricted ionic environments, i.e. between cations and anions.* Using especially designed ILs namely 1,2,3-trimethyl-1*H*-imidazol-3-ium imidazol-1-ide (MMMI·Im) and 3-*n*-butyl-1,2-dimethyl-1*H*-imidazol-3-ium imidazol-1-ide (BMMI·Im), the structure and function of water has been determined in condensed, solution and gas phases by X-Ray diffraction studies, NMR, molecular dynamic simulations (MDS) and DFT calculations. In the solid state the water molecule is trapped inside the ionic network (constitute of contact ion pairs formed by π^+-π^- interaction) through strong H-bonds involving the water hydrogens and the nitrogens of two imidazolate anions forming a guest@host supramolecular structure. A similar structural arrangement was corroborated by DFT calculations and MDS. The presence of a guest@host species (H_2O@ILpair) is maintained to a great extends even in solution as detected by ^{1}H-^{1}H NOESY-experiments of the ILs dissolved in solvents with low and high dielectric constants. This confined water catalyses the H/D exchange with other substrates containing acidic-H such as chloroform.

Introduction

Neat imidazolium based ionic liquids (ImILs) are highly organized 3-D materials in the condensed phase with a broad range of applications in chemistry, physics, materials and biosciences.[1-4] The physico-chemical properties at the nanoscopic level of ImILs have been ascribed as a result of various bond forces namely: electrostatic, hydrogen bonding and dispersive forces. The structural organization of ImILs is mainly controlled by an intricate interplay of intermolecular interactions between anions and cations. In particular, ILs based on the imidazolium cation are compounds in which π^+-π^+ stacking interactions among the imidazolium rings[5] may also be involved,[6, 7] and their interaction energy depends on the different orientations adopted by the imidazolium rings.[8-10] Thus, all these non-bonding interactions should be recognized as a key component in the local structure of imidazolium based compounds and they have been subject of several theoretical[11-15] and experimental studies.[16-24] However, experimentally pure ILs are extremely difficult to obtain, especially water-free ones.[25, 26] It is well recognized that the presence of water may dramatically effect macroscopic physico-chemical properties of ionic liquids[27] such as viscosity, density,[28] diffusion, ionic mobility[29] and gas solubility.[30-32] On the microscopic scale, computer simulations on IL/water mixtures revealed the influence of water on the IL structure and dynamical features.[14, 33, 34] It is therefore reasonable also to expect that even trace amounts of water may have a profound impact at the nanoscopic level on the organization and reactivity of these fluids. However, the function of water *within this confined space and restricted ionic environments, i.e. between imidazolium cations and anions,* has not yet been experimentally firmly established.

The most important forces, present in the supramolecular structure of neat imidazolium based ILs holding multiple ion pairs together, consist mainly of dispersion interactions, electrostatics and hydrogen bonds. Water molecules affect these interactions.[35, 36] Thus, the structure and dynamics of water traces in imidazolium based ILs[37] can be regarded as a consequence of a guest that is non-covalently bound to the ion pairs network, i.e. the host forming a guest@host species (H_2O@ILpair). As in many guest@host complexes, the guest (H_2O) is relatively small compared with the host (IL pair) and they should behave as a unit. Moreover, the IL ion pairs may provide a cage that completely surrounds the guest

[a] Institute of Chemistry, UFRGS, Avenida Bento Gonçalves, 9500 Porto Alegre 91501-970 RS Brazil
[b] School of Chemistry, University of Nottingham, University Park, NG7 2RD, Nottingham UK

Electronic Supplementary Information (ESI) available: NMR spectra (PDF), crystal data of MMMI·Im (CIF), DFT and MDS details (PDF). See DOI: 10.1039/x0xx00000x

(guest@cage) or provide a cavity (guest@cavity) that partially surrounds the guest.[38-40] Assuming this hypothesis, we have designed ImILs in which traces of water are experimentally investigated in the condensed phase and in solution by NMR experiments. In particular, ImILs associated with the imidazolate anion (Figure 1) display the desired structural and electronic features such as possible π⋯π cation-anion interactions in solution as well as nitrogen basic sites that can easily accommodate water molecules by hydrogen bonds.

For this study, we have chosen the symmetric 1,2,3-trimethylimidazolium cation (MMMI) that is solid and crystalline at room temperature (RT) yielding simplified NMR spectra. In addition, we employed the non-symmetric 1,2-dimethyl-3-*n*-butyl imidazolium BMMI analogue that possesses a better solubility in organic solvents.

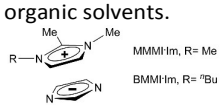

Figure 1. ImILs associated with the imidazolate anion.

We report herein our experimental and theoretical results revealing the impact of water in this confined and restricted space forming a guest@host complex by the interaction with the contact ion-pair (imidazolium cation-imidazolate anion).

Results and discussion

Synthesis and X-ray structure of the water@ImIL complex. The MMMI·Im (mp= 36 °C) and BMMI·Im (mp= 23 °C) ILs have been prepared in quantitative yield by the reaction of MMMI·OH and BMMI·OH (prepared by anion exchange of chloride salts and NaOH using an anionic Amberlite resin), respectively with imidazole. Crystals of MMMI·Im suitable for X-ray diffraction have been obtained from the slow evaporation of MeCN solution. The structure of [MMM·Im]·[H2O] is illustrated in Figure 2 together with selected bond angles and distances. Crystal data are summarized in Table S1 of the supporting information. It is clear from Figure 2a that each imidazolium cation is in relative strong contact with the imidazolate anion through π^{+}-π^{-} interaction.

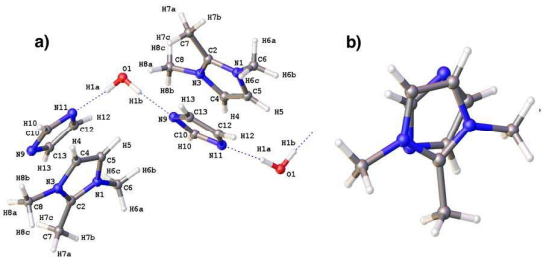

Figure 2. X-Ray structure of MMMI·Im containing the water H-bonded (trapped) in the IL network (a) and the quasi-staggered conformation of the imidazolium-imidazolate ion pair (b). (O1H1AN11= 172 (2)º, O1-N11= 2.780(16) Å; O1H1BN9= 170(2)º, O1N9= 2.8335(17) Å).

The two five-membered rings are in a quasi-staggered conformation in which the cation's ring moiety is located in an anti-parallel position to the ring of the imidazolate anion (Figure 2b). The most relevant aspect is the presence of water molecules which are "trapped" inside the ionic network (constitute of contact ion pairs) through strong H-bonds involving one H of water and the nitrogens (N9 and N11) of two imidazolate anions (Figure 2a).

Structure and behaviour of the water@ImIL in solution. The ^{1}H NMR spectra of both ILs from Figures S9-S18 in the supporting information clearly present a decrease in the intensity of the C7 hydrogen signals (originally singlet at around 2.48 ppm) in various solvents ($CDCl_3$, CD_3OD, CD_3CN, [D_6]DMSO and D_2O) and the appearance of a triplet and quintet corresponding to CH_2D and CHD_2 (around 2.46 and 2.44 ppm). In the ^{13}C NMR spectrum (Figures S6 and S8 in the supporting information), we observed a triplet and a septuplet around 7.6 ppm corresponding to the C7 carbon coupled to D. Some H/D exchange at the cation's C4/C5 position has also been detected but the deuteration occurs preferentially at C7 (see Table 1) within 1h. In principle, this observation might be explained by the solvated imidazolate anion acting as a base catalyst. However, in that case the reaction should be more efficient in D_2O since it is well known that D incorporation is by far more difficult to achieve in aprotic solvents such as $CDCl_3$ than in protic polar solvents like D2O, partly due to the limited strength of bases in a low dielectric constant medium.

Table 1. Degree (%)[a] of deuteration of the C7 and C4-C5 hydrogens of the imidazolium cation (0.2 M) in different solvents after 1h in solution.[b]

Entry	Solvent	IL	C7	C4/C5
1	$CDCl_3$	MMMI·Im	88	12
2	$CDCl_3$	BMMI·Im	91	15
3	CD_3OD	MMMI·Im	91	34
4	CD_3OD	BMMI·Im	97	16
5	CD_3CN	MMMI·Im	90	80
6	CD_3CN	BMMI·Im	31	23
7	[D_6]DMSO	MMMI·Im	3	3
8	[D_6]DMSO	BMMI·Im	8	0
9	D_2O	MMMI·Im	32	27
10	D_2O	BMMI·Im	14	17

[a] Determined by ^{1}H NMR spectroscopy by the integral of the singlet of the C7 methyl group and the C4/C5 hydrogen atoms. [b] Reaction conditions: RT, without stirring, 0.2 M. Dieletric constants: $CDCl_3$ (4.89); CD_3OD (32.66); CD_3CN (37.5); [D_6]DMSO (46.45) and D_2O (78.36).

Most important, the ^{1}H-^{1}H NOESY experiments indicate the presence of intimate contact ion pairs in CD_3CN and [D_6]DMSO at relative low concentrations (0.2 M), and even in D_2O, although at higher concentrations (1 M) (see Figures S29 and S30 and S35 supporting information). These results suggest that the H/D reaction is probably catalysed by the contact ion-pair[41] of MMMI·Im and BMMI·Im as already observed for BMMI ILs associated with hydrogen carbonate and prolinate anions.[42] However, in the case of the imidazolate anion studied here strongly interacting with imidazolium cations, there is no "extra" basic site to perform the catalytic H/D exchange reaction. Note that in most of the cases traces of

water are necessary to activate the catalytic active species (Scheme 1).

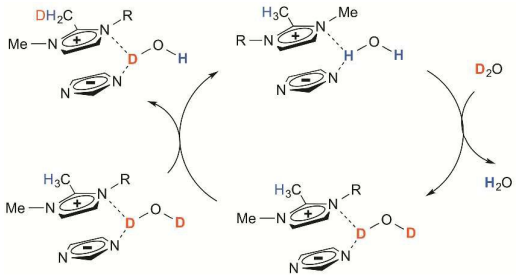

Scheme 1. Proposed reaction paths for the H/D exchange promoted by the confined water in the contact ionic pair**.**

Moreover, in the case of [D_6]DMSO, in which H/D exchange degree is lower than in the other used organic solvents, we observed the water (at 7.27 ppm for MMMI·Im and at 4.58 ppm for BMMI·Im) signal in the ^{1}H NMR spectra (see Figure S15-S16 in the supporting information). Note that this signal can hardly be detected in the case of the other wet organic solvents suggesting a very rapid H/D exchange of the D-solvents and H_2O leading to D_2O. Very important, the HDO signal could be observed in the ^{1}H-^{1}H NOESY experiments (see Figure 3 and Figure S30-S33 in the supporting information) and the cross over peaks indicate that this species is exchanging H with the C7-methyl group.

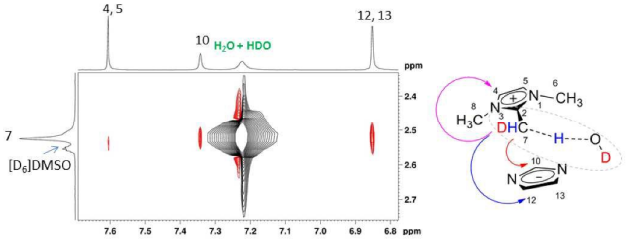

Figure 3. ^{1}H-^{1}H NOESY cross-peak of C7 and C4/C5; C12/13 and C10 and H_2O/HDO of the supramolecular complex [MMMI·Im]·[HDO] in [D_6]DMSO (1 M).

In addition, the ^{1}H-^{1}H NOESY results exhibit cation–anion interaction patterns with higher cross-peak intensity, corresponding to higher relative cross-relaxation rates, between HDO and the hydrogens of the three methyl groups of the imidazolium cation (Figure 4).

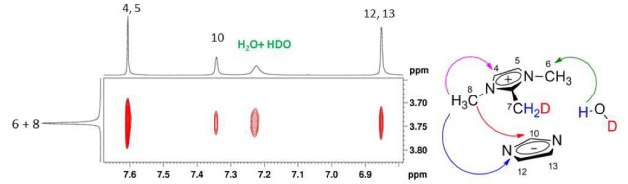

Figure 4. ^{1}H-^{1}H NOESY cross-peak of NCH_3 (C6 and C8) and C4/C5; C12/13 and C10 and H_2O/HDO of the supramolecular complex [MMMI·Im]·[HDO] in [D_6]DMSO (1 M).

These interaction patterns correspond to the preferential sites for cation–anion interactions, in which water is located close to the imidazolium substitutions C6, C7, and C8 and also close to one the N of the imidazolate anion. Such structural arrangement is similar to the solid state X-Ray diffraction structure and the geometrics optimized by DFT calculations (see below). Therefore, the confined water in this restricted ionic environment is activated acting as a catalyst base for the H/D exchange reaction (Scheme 1). This is a typical case of guest@host complexes, in which a relatively small guest (H_2O) behaves as a unit with the host (IL pair). MDS corroborated the existence of the π^+-π^- contact ion pairs and their interaction with water (see below). Therefore, it appears quite probable that the confined water is mediating the intermolecular H/D exchange between the D-solvent and the H of the C-7 Me group of the imidazolium cation, explaining the preferential H/D exchange at C-7 rather than at C4/C5 (see Table 1).

It is also worth to note that the addition of H_2O (25 µL) to the NMR tube containing MMMI·Im in [D_6]DMSO (1 M) shifts the water proton signal from 7.18 ppm to 4.83 ppm. We have not been able to detect the signal of residual H_2O in [D_6]DMSO that is usually observed at 3.33 ppm[43] in the ^{1}H NMR Spectrum (see Figure 5). This behaviour was confirmed by de ^{2}H NMR (see Figure S24) in which the signal of water is shifted from 6.77 to 4.82 ppm after the addition of H_2O.

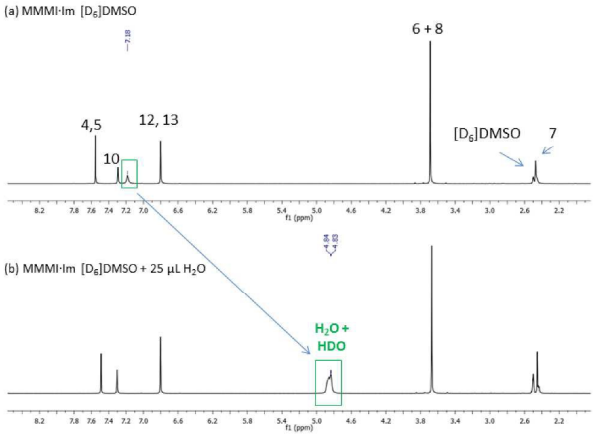

Figure 5. ^{1}H NMR spectra of MMMI·Im in [D_6]DMSO (1 M) in 72h: without water addition (a), addition of 25 µL H_2O (b).

In addition, such an activation of water was corroborated by the facile H/D exchange between MMMI·Im dissolved in D_2O, dried, and afterwards treated by $CHCl_3$ furnishing $CDCl_3$ (see Scheme 2 and Figures S19- S22 in the supporting information).

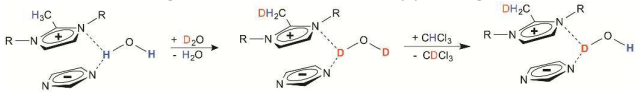

Scheme 2. IL Confined water as D transfer agent.

In these cases, in which the ImILs/water interaction could be detected by NMR, the IL seems to be ''frozen'' with the water molecule in an IL cage. These arrangements might be represented by a guest@cage, because the water is completely surrounded by the guest during this short time

period (NMR time scale).[40] However, on longer time scales, the IL pairs can separate to produce free volume through which the guest (H_2O) can escape from the IL ion pairs cage (Scheme 3).

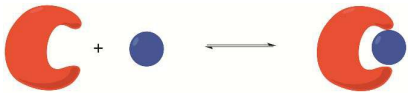

Scheme 3. Topological view for the formation of the monomeric guest (water - blue)@host (contact ion pair – red) complex in " wet" solvents.

The same supramolecular model can be extended to other guests than water such as in the case of carbon dioxide for which it has been reported that the cooperative network (dispersive forces and hydrogen bonds) of classical imidazolium ILs BMI·BF_4 and BMI·PF_6 is only marginally disrupted and the cation-anion contact ion pair is unaffected by the inclusion of CO_2.[44, 45] The formation of liquid clathrate in ionic liquid-aromatic mixtures can be also described as guest@host complex formation.[46] Moreover, the same water function can explain the oxidation of iron nanoparticles to FeO nanoparticles in oxygen free ImILs,[47] the stabilisation of enzymes at high temperatures,[48] or the H/D exchange in deuterated solvents of classical 1-alkyl-3-methyl imidazolium ILs,[49] for example.

DFT calculations. The ion pair has been optimized first without the inclusion of a water molecule employing DFT (Figure 6a and Figure S36 in the supporting information). Two stable ions pairs have been obtained, one containing an anti-parallel π^+-π^- cation-anion stack, the other with an almost parallel π^+-π^- cation-anion stacking. The anti-parallel configuration (Figure 6a) is energetically slightly favoured by 1.9 kcal.mol^{-1}, presenting a value of 93.9 kcal.mol^{-1} for the cation-anion interaction.

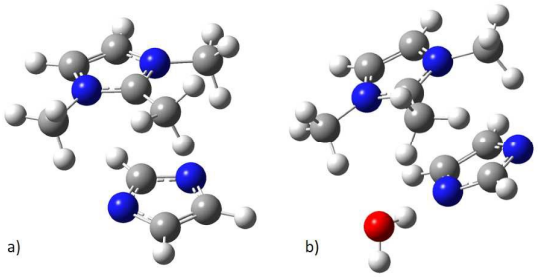

Figure 6. Optimized structure obtained by DFT of ionic pair of MMMI·Im (a) and the ionic pair MMMI·Im (anti-parallel displaced) with water (b).

A single water molecule has been added to these ion pair configurations. The optimized final structures are displayed in Figures 6b and S36 (supporting information). It becomes evident that both configurations maintained the π^+-π^- stacking. However, starting with the parallel π^+-π^- stack, we observed a tendency to anti-parallelize the two ring systems whereas the anti-parallel π^+-π^- stack is conserved more stable by 1.3 kcal.mol^{-1}, and very similar to the X-ray structure from Figure 2.

Intra-ionic structural parameters (bond lengths, bond angles and torsion angles) are summarized in Tables S9-S11 (supporting information) and compared with X-ray data. Final coordinates for all the calculated geometries are presented in Tables S2-S8 from the supporting information.

The interaction energy of the ion pair with the water molecule (17.3 kcal.mol^{-1}) indicates strong hydrogen bonding of the water proton to the anion's nitrogen atom. The corresponding distance of 1.66 Å is much shorter than in the X-ray structure (1.89 and 1.95 Å) due to the fact that only a single ion pairs has been considered in the calculation, whereas the water molecules bridges two ion pairs in the solid state. However, the O-H-N angles in the DFT and crystal structures are in nice agreement (168.5° and 170°, respectively). It is worth to mention that the distances between MMMI's methyl groups and the water oxygen correspond to weak hydrogen bonds.

Molecular dynamics simulations. We have performed MDS on the MMMI·Im and BMMI·Im ion pairs coordinated by a single water molecule in chloroform. Several structural aspects of these aggregates are described below.

In Figure 7, we illustrate the time evolution of the shortest distances between any atom of the cation and the anion as well as the water molecule. Along the simulation time of 60 ns, Figure 7 demonstrates that the ion pair formed by the imidazolate anion with both cations remains stable in chloroform. In addition, the water molecule maintains contact with the ion pairs during the simulation. Figure 7 reveals only short periods of larger separations between the cations and the water molecule. Radial pair distribution functions g(r) for all the atom pairs (cation-anion, cation-water, anion-water) have been computed from the last 20 ns of the simulation containing the MMMI·Im/water system and for the period between 20 and 40 ns of the BMMI·Im/water simulation.

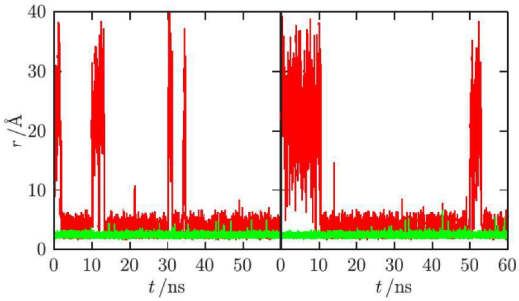

Figure 7. Time evolution of the minimum distances between the cation and anion (green) and between the cation and the water molecule (red) in chloroform solution. Left panel: MMMI·Im, right panel: BMMI·Im.

These functions correspond to probability distributions for interatomic distances in the simulated systems with the reference being an ideal gas at the same number density.

From the X-ray structure and the DFT calculations discussed above, the water coordination has been revealed due to hydrogen bonding between the water protons and the negatively charged nitrogen atoms of the anion. In Figure 8,

we present the g(r) for these nitrogen atoms and the water atoms. These correlations exhibit the features typical for strong hydrogen bonding with N-H distances of 1.84 Å (X-ray: 1.89 and 1.95 Å, DFT: 1.66 Å) and N- O distances of 2.75 Å (X-ray: 2.78 and 2.83 Å, DFT: 2.73 Å). The integrals of the first sharp peaks in these functions yield 0.5 hydrogens and oxygens consistent with the picture that on average one of the water hydrogens is strongly coordinated to one of the anion's nitrogen atoms. Figure 8 also reveals that these findings are independent on the choice of the cation.

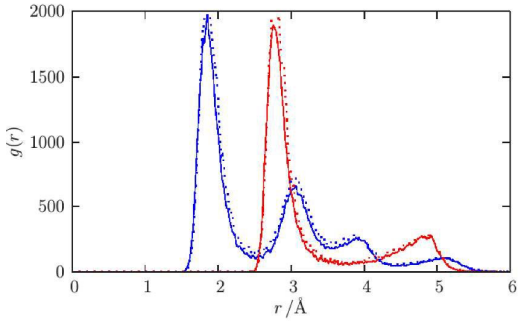

Figure 8. Radial pair distribution functions between the nitrogen atoms of the anion and the protons (blue) and oxygens (red) of the water molecule. Full lines: MMMI cation, dotted lines: BMMI cation.

From the spatial distribution functions (see graphical abstract), the X-ray structure and the DFT calculations, it becomes evident that the ion pair is maintained to a certain degree by π-stacking even when the water molecules are coordinated. These configurations are characterized by the H-H contacts obtained from NMR data as illustrated in Figures 3 and 4. In Figure 9, we depict the H-H pair distributions for the protons of cation and anion with water hydrogens for the MMMI system, in Figure S37 (supporting information) for the BMMI system. These function present sharper peaks for correlations of the water protons with the anion's hydrogens with the shortest distances below 3 Å observed for the H12 and H13. The g(r) involving the cation is very broad with lower amplitudes and no significant differences between the various hydrogens. However, peak maxima at 3.5 Å correspond well with the detected correlations of these protons with water hydrogens in the NMR signals from Figures 3 and 4.

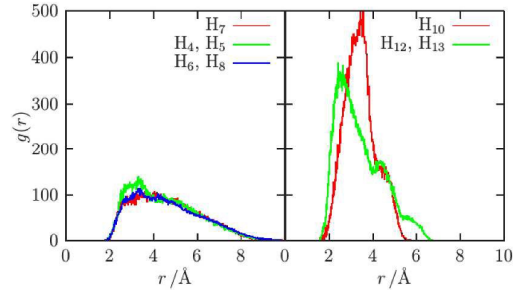

Figure 9. Radial distribution functions for distances between the water protons and the hydrogens of the cation (left panel) and the anion (right panel) for the MMMI system.

Comparing the cation coordination of the water protons from Figures 9 and S37, we find larger amplitudes in the BMMI system for the protons at C4 and C6 indicating the steric interference of the butyl substitution at C1 for water contacts at the hydrogens of C5 and C8. NMR has also revealed these differences as demonstrated by Figure S31.1.

In Figures 10 and S38, we depicted these functions for the ion pairs focusing on correlations between the cation's and the anion's hydrogen atoms. Note that the g(r) for the ion pairs from these figures are not affected by the added water molecule. We compared these functions with those obtained from simulations of the ion pair without water molecule in chloroform (not shown here) and could not find any differences. Thus, the water molecule is not intercalated between cation and anion.

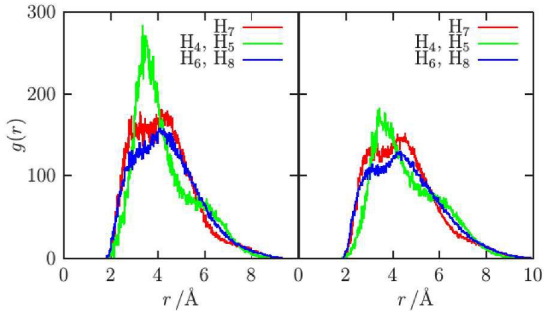

Figure 10. Radial distribution functions for distances between the cation's hydrogens and the anion's H10 (left panel) and the anion's H12 and H13 (right panel) in the MMMI system.

These figures exhibit short-range contacts between all the combinations of hydrogen atoms as observed in the NMR spectra. Distributions with the anion's H10 proton exhibit larger amplitudes than those involving the proton's H12 and H13. The g(r) involving the cation's ring protons H4 and H5 are somewhat sharper and more intense the correlations for the methyl protons H6, H7, and H8. Figure S38 demonstrates that the butyl group affects these functions furnishing more pronounced correlations at the N-methyl side of the cation as observed above in the correlations with the water molecule.

Conclusions

Water traces in ImILs can be regarded as guest@host supramolecular complexes with the water molecules trapped inside the ionic network (constitute of contact ion pairs formed by [+]-[-] interaction) through strong H-bonds involving the water hydrogens and the nitrogens of imidazolate anions. These water interactions strongly interfere on the supramolecular organization of the fluids. The supramolecular guest@host complex is maintained in solution even in solvents with high dielectric constants such as DMSO. The supramolecular organization (H_2O@ILpair) has been corroborated by both experimental (NMR) and computational chemistry. The water is confined in this restricted ionic environment and behaves as base catalyst promoting the H/D exchange reaction with both, the hydrogens of the

imidazolium cation, and as well as other acidic compounds. This model might be very useful to rationalize and predict the behaviour of physical and chemical processes occurring in "wet" ionic liquids. Therefore, the presence of activated water in ILs should be taken into consideration when employing and analysing the physico-chemical properties of these fluids.

Experimental

Materials and instruments. All reagents were obtained from Sigma-Aldrich and used without purification. Deuterated solvents were purchased from Cambridge Isotope Laboratories. The NMR samples were prepared by dissolving the corresponding ionic liquid in 500 µL of deuterated solvent and the analysis was carried out at 25 °C. Infrared spectra were performed with an ALPHA Bruker FT-IR spectrometer. High resolution mass spectrometry electrospray ionization (HRMS-ESI) data, in a positive and negative mode, were collected using a Micromass Q-Tof instrument. Samples were infused by a 100 µL syringe at a flow rate of 30 µL min^{-1} for all samples. Typical operating conditions were: a capillary voltage of 2980 V, a sample cone voltage of 30 V, an extraction cone voltage of 3.0 V, and a desolvation gas temperature of 60 °C. N_2 was used as the desolvation gas and deionized water as the solvent of the samples.

Synthesis of 1,2,3-trimethyl-1H-imidazol-3-ium iodide (MMMI·I):[50] Methyl iodide (14.91 g, 105 mmol) was added at room temperature under magnetic stirring to 1,2-dimethylimidazole (9.61 g, 100 mmol), dissolved in acetonitrile (30 mL). The exothermic reaction was controlled with an external water-ice bath and the reaction mixture was stirred for further 45 min. The resulting crystalline solid was filtered, washed with small portions of cold acetonitrile and dried under reduced pressure, leaving the desired 1,2,3-trimethyl-1*H*-imidazol-3-ium iodide as colorless crystals (20.94 g, 88 % yield). Melting point: 310-314 °C (dec.). ^{1}H NMR (400 MHz; D_2O): δ 7.37 (s, 2H), 3.84 (s, 6H), 2.66 (s, 3H).

Synthesis of 3-n-butyl-1,2-dimethyl-1H-imidazol-3-ium chloride (BMMI·Cl): The ionic liquid was prepared according to known procedures,[51] to give a white crystalline solid. Melting point: 94-96 °C. ^{1}H NMR (400 MHz; $CDCl_3$): δ 7.90 (d, 1H, *J* = 1.9), 7.66 (d, 1H, *J* = 1.9), 4.28 (t, 2H, *J* = 7.3), 4.07 (s, 3H), 2.85 (s, 3H), 1.81 (m, 2H), 1.39 (m, 2H), 0.96 (t, 3H).

General procedure of anion exchange: The corresponding imidazolium salt (20 mmol) was dissolved in a minimum amount of water and eluted through an ion exchange resin column (Amberlite IRA 400, 100mL, basic form). Imidazole (1.36 g, 20 mmol) was added to the resulting aqueous corresponding imidazolium hydroxide solution and the water was evaporated under reduced pressure.

1,2,3-trimethyl-1H-imidazol-3-ium imidazolate (MMMI·Im): 1,2,3-trimethyl-1*H*-imidazol-3-ium iodide (4.76 g, 20 mmol) was eluted through the column to resulting a yellow semisolid residue that has been re-crystallized with acetonitrile/ethyl acetate, giving very hygroscopic pale yellow crystals (3.34 g, 94 % yield). ^{1}H NMR (400 MHz; D_2O): δ 7.2 (s, 1H), 6.85 (s, 2H), 6.71 (s, 2H), 3.32 (s, 6H), 2.05 (m, 3H); ^{13}C NMR (101 MHz, D_2O) δ 144.0, 139.0, 123.0, 121.4, 34.1, 7.4. ES-MS(+) (m/z) elem. anal. calcd. for: $C_6H_{11}N_2^+$ 111.0922; found 111.0785. ES-MS(-) (m/z) elem. anal. calcd. for: $C_3H_3N_2^-$ 67.0302; found 67.0600.

3-*n*-butyl-1,2-dimethyl-1*H*-imidazol-3-ium imidazolate (BMMI·Im):[52] 3-*n*-butyl-1,2-dimethyl-1*H*-imidazol-3-ium chloride (3.77 g, 20 mmol) was eluted through the column to resulting an orange semisolid (4.05 g, 92 % yield). ^{1}H NMR (400 MHz, D_2O) δ 7.63 (s, 1H), 7.24 (s, 1H), 7.21 (s, 1H), 7.02 (s, 1H), 4.00 (t, 2H, *J* = 7.3), 3.66 (s, 3H), 2.47 (s, 3H), 1.69 (m, 2H), 1.25 (m, 2H), 0.86 (t, 3H, *J* = 7.4). ^{13}C NMR (101 MHz, D_2O) δ 143.8, 137.3, 122.3, 121.9, 120.5, 47.7, 34.3, 30.8, 18.7, 12.7, 8.4.

NMR Experiments. All NMR experiments were performed on a Bruker Avance 400 spectrometer equipped with a BBO 5 mm probe with z-gradient operating at 400.06 MHz for ^{1}H, and 100.46 MHz for ^{13}C. Spectra were obtained at a probe temperature of 298 K referenced to Me_4Si under conditions for ^{1}H (spectral width 6400 Hz with 32 K data points and zero filled to 128 K to give a digital resolution of 0.05 Hz/pt). Chemical shifts were reported in parts per million (ppm, δ) and referenced to solvent pick; $CDCl_3$ (δ 7.26 in ^{1}H and 77.0 in ^{13}C), D_2O (δ 4.79 in ^{1}H) [D_6]DMSO (δ 2.50 in ^{1}H and 39.43 in ^{13}C), CD_3CN, (δ 1.94 in ^{1}H and 1.39 in ^{13}C) and CD_3OD (δ 3.31 in ^{1}H and 49.00 in ^{13}C). For ^{1}H NMR spectra, multiplicities are reported as s (singlet), d (doublet), t (triplet), q (quartet), quint (quintet), sex (sextet), m (multiplet), br (broad), or a combination of these. The 2D-NOESY spectra were recorded using 256 F1 increments and 4096 F2 complex points. The experimental data sets were zero-filled in both the F1 and F2 dimension to form a 4096 X 512 data matrix. The mixing time was 800 ms and the delay between two experiments (d_1) was 2 s. The resulting data were processed using a sine bell transformation function (implemented in the Topspin2.1 software) in both dimensions prior to Fourier transformation.

X-Ray Diffraction analysis. Single crystals of $C_9H_{16}N_4O$ [MMMI·Im] were obtained from slow evaporation of a MeCN solution at RT. A suitable crystal was selected and [in fomblin film on a micromount] on a SuperNova, Dual, Cu at zero, Atlas diffractometer. The crystal was kept at 120(2) K during data collection. Using Olex2,[53] the structure was solved with the olex2.solve[54] structure solution program using Charge Flipping and refined with the ShelXL[55] refinement package using Least Squares minimization. Crystal Data for $C_9H_{16}N_4O$ (*M* =196.26 g.mol^{-1}): monoclinic, space group $P2_1/n$ (no. 14), *a* = 7.3864(4) Å, *b* = 12.0203(7) Å, *c* = 12.5938(7) Å, *β* = 103.725(6)°, *V* = 1086.24(11) Å^3, *Z* = 4, *T* = 120(2) K, µ(CuKα) = 0.669 mm^{-1}, *Dcalc* = 1.200 g/cm^3, 4439 reflections measured (10.316° ≤ 2Θ ≤ 149.746°), 2149 unique (R_{int} = 0.0296, R_{sigma} = 0.0272) which were used in all calculations. The final R_1 was 0.0509 (I > 2σ(I)) and wR_2 was 0.1456 (all data).

DFT calculations. Considering that the studied ionic pairs were significantly influenced by dispersive interactions, Density Functional Theory (DFT) calculations, using the long-range corrected wB97X-D hybrid density functional were realized.[56] This functional furnishes a good accuracy for calculations of thermodynamic properties for bonded systems including non-bonded interactions. The spAug-cc-pVTZ basis set was used for

all atoms. This basis set is comprised by the cc-pVTZ basis set[57] augmented with s and p diffuse functions. Geometry optimizations were conducted using the default algorithm with the TIGHT convergence criteria, followed by frequency calculations to ensure the nature of the stationary points. All calculations were performed with the Gaussian 09 package.[58]

Molecular Dynamics Simulations. We have performed molecular dynamics (MD) computer simulations on single ion pairs and a single added water molecule in the solvent chloroform. We considered ion pairs of the MMMI and BMMI cations with the imidazolate anion. Force field parameters for the ions have been established within the AMBER directives as described in [59] from geometries optimized quantum-mechanically at the B3LYP//RHF6-311G(d,p) (cations) and B3LYP//RHF6-311++G(d,p) (imidazolate) levels. Intramolecular parameters for the methyl group at the cation's C7 have been defined as in the toluene molecule.

The simulations have been performed with the GROMACS 4.5.5 package.[60] We employed the NpT ensemble maintaining the temperature at 298 K by velocity rescaling[61] and the pressure at 1 bar with the Parrinello-Rahman barostat.[62] Bond lengths were constrained by the LINCS[63] and, in the case of the water molecule, by the SETTLE algorithms.[64] Equations of motion have been integrated using a time step of 0.002 ps. The PME[65] method was utilized to correct for long-range electrostatic interactions. A cut-off distance of 13 Å has been applied.

The chloroform solvent was obtained as a cubic box containing 1000 molecules from the GROMACS Molecule & Liquid Data Bases[66] within the GAFF parameterization.[67]

The TIP3P model[68] was employed for the water molecule. Starting configurations have been generated simulating a single cation with the imidazolate anion for 100 ps in a cubic box with dimensions perfectly matching the size of the solvent box. Afterwards, single water molecule was added before solvating the system with the chloroform. If necessary, a short energy minimization procedure was applied before simulating for 60 ns. Density, inter- and intramolecular energy terms were monitored during the simulations. The convergence of these properties indicated that the systems were equilibrated within a few nanosceconds.

Acknowledgements

Thanks are due to CNPq, CAPES and FAPERGS (Brazil) for partial financial support.

Notes and references

1. J. Dupont, *Acc. Chem. Res.*, 2011, **44**, 1223-1231.
2. S. J. Zhang, J. Sun, X. C. Zhang, J. Y. Xin, Q. Q. Miao and J. J. Wang, *Chem. Soc. Rev.*, 2014, **43**, 7838-7869.
3. R. Ferraz, L. C. Branco, C. Prudencio, J. P. Noronha and Z. Petrovski, *ChemMedChem*, 2011, **6**, 975-985.
4. P. A. Hunt, C. R. Ashworth and R. P. Matthews, *Chem. Soc. Rev.*, 2015, **44**, 1257-1288.
5. R. P. Matthews, T. Welton and P. A. Hunt, *Phys. Chem. Chem. Phys.*, 2014, **16**, 3238-3253.
6. J. S. Wilkes and M. J. Zaworotko, *J. Chem. Soc., Chem. Commun.*, 1992, DOI: 10.1039/C39920000965, 965-967.
7. A. Garcia-Saiz, I. de Pedro, P. Migowski, O. Vallcorba, J. Junquera, J. A. Blanco, O. Fabelo, D. Sheptyakov, J. C. Waerenborgh, M. T. Fernandez-Diaz, J. Rius, J. Dupont, J. A. Gonzalez and J. R. Fernandez, *Inorg Chem*, 2014, **53**, 8384-8396.
8. A. Mele, G. Romanò, M. Giannone, E. Ragg, G. Fronza, G. Raos and V. Marcon, *Angew. Chem. Int. Ed.*, 2006, **45**, 1123-1126.
9. H. Li, J. A. Boatz and M. S. Gordon, *J. Am. Chem. Soc.*, 2008, **130**, 392-393.
10. A. R. Choudhury, N. Winterton, A. Steiner, A. I. Cooper and K. A. Johnson, *J. Am. Chem. Soc.*, 2005, **127**, 16792-16793.
11. Y. Wang and G. A. Voth, *J. Am. Chem. Soc.*, 2005, **127**, 12192-12193.
12. B. A. Marekha, O. N. Kalugin and A. Idrissi, *Phys. Chem. Chem. Phys.*, 2015, **17**, 16846-16857.
13. M. L. Sha, H. Z. Dong, F. B. Luo, Z. F. Tang, G. L. Zhu and G. Z. Wu, *J. Phys. Chem. Lett.*, 2015, **6**, 3713-3720.
14. C. Spickermann, J. Thar, S. B. C. Lehmann, S. Zahn, J. Hunger, R. Buchner, P. A. Hunt, T. Welton and B. Kirchner, *J. Chem. Phys.*, 2008, **129**.
15. B. Kirchner, F. Malberg, D. S. Firaha and O. Holloczki, *J Phys Condens Matter*, 2015, **27**, 463002.
16. D. A. Turton, J. Hunger, A. Stoppa, G. Hefter, A. Thoman, M. Walther, R. Buchner and K. Wynne, *J. Am. Chem. Soc.*, 2009, **131**, 11140-11146.
17. J. Dupont, *J. Braz. Chem. Soc.*, 2004, **15**, 341-350.
18. F. H. Allen, *Acta Crystallogr. Sect. B: Struct. Sci.*, 2002, **58**, 380-388.
19. I. de Pedro, A. García-Saiz, J. Dupont, P. Migowski, O. Vallcorba, J. Junquera, J. Rius and J. Rodríguez Fernández, *Cryst. Growth Des.*, 2015, **15**, 5207-5212.
20. C. Roth, T. Peppel, K. Fumino, M. Köckerling and R. Ludwig, *Angew. Chem. Int. Ed.*, 2010, **49**, 10221-10224.
21. B. A. Marekha, O. N. Kalugin, M. Bria and A. Idrissi, *Phys. Chem. Chem. Phys.*, 2015, **17**, 23183-23194.
22. S. R. Prabhu and G. B. Dutt, *J. Phys. Chem. B*, 2015, **119**, 10720-10726.
23. M. A. Ab Rani, A. Brant, L. Crowhurst, A. Dolan, M. Lui, N. H. Hassan, J. P. Hallett, P. A. Hunt, H. Niedermeyer, J. M. Perez-Arlandis, M. Schrems, T. Welton and R. Wilding, *Phys. Chem. Chem. Phys.*, 2011, **13**, 16831-16840.
24. T. Koddermann, C. Wertz, A. Heintz and R. Ludwig, *Angew. Chem. Int. Ed.*, 2006, **45**, 3697-3702.
25. J. P. Armstrong, C. Hurst, R. G. Jones, P. Licence, K. R. J. Lovelock, C. J. Satterley and I. J. Villar-Garcia, *Phys. Chem. Chem. Phys.*, 2007, **9**, 982-990.
26. K. R. J. Lovelock, A. Deyko, P. Licence and R. G. Jones, *Phys. Chem. Chem. Phys.*, 2010, **12**, 8893-8901.
27. K. R. Seddon, A. Stark and M. J. Torres, *Pure Appl. Chem.*, 2000, **72**, 2275-2287.
28. J. Jacquemin, P. Husson, A. Padua and V. Majer, *Green Chem.*, 2006, **8**, 172-180.
29. U. Schröder, J. D. Wadhawan, R. G. Compton, F. Marken, P. A. Z. Suarez, C. S. Consorti, R. F. de Souza and J. Dupont, *New J. Chem.*, 2000, **24**, 1009-1015.
30. D. Fu, X. Sun, J. Ou and S. Zhao, *J. Chem. Eng. Data*, 2006, **51**, 371-375.

31. N. Hollingsworth, S. F. Taylor, M. T. Galante, J. Jacquemin, C. Longo, K. B. Holt, N. H. de Leeuw and C. Hardacre, *Angew. Chem. Int. Ed.*, 2015, **54**, 14164-14168.
32. S. F. R. Taylor, C. McCrellis, C. McStay, J. Jacquemin, C. Hardacre, M. Mercy, R. G. Bell and N. H. de Leeuw, *J. Solution Chem.*, 2015, **44**, 511-527.
33. S. Feng and G. A. Voth, *Fluid Phase Equilib.*, 2010, **294**, 148-156.
34. T. Mendez-Morales, J. Carrete, O. Cabeza, L. J. Gallego and L. M. Varela, *J Phys Chem B*, 2011, **115**, 6995-7008.
35. L. Cammarata, S. G. Kazarian, P. A. Salter and T. Welton, *Phys. Chem. Chem. Phys.*, 2001, **3**, 5192-5200.
36. M. Brehm, H. Weber, A. S. Pensado, A. Stark and B. Kirchner, *Phys. Chem. Chem. Phys.*, 2012, **14**, 5030-5044.
37. P. Stange, K. Fumino and R. Ludwig, *Angew. Chem. Int. Ed.*, 2013, **52**, 2990-2994.
38. J. M. Lehn, *Angew. Chem. Int. Ed.*, 1988, **27**, 89-112.
39. J. M. Lehn, *Angew. Chem. Int. Ed.*, 1990, **29**, 1304-1319.
40. N. J. Turro, *Proc. Natl. Acad. Sci. U. S. A.*, 2005, **102**, 10765-10765.
41. H. K. Stassen, R. Ludwig, A. Wulf and J. Dupont, *Chem. Eur. J.*, 2015, **21**, 8324-8335.
42. M. Zanatta, A. L. Girard, N. M. Simon, G. Ebeling, H. K. Stassen, P. R. Livotto, F. P. dos Santos and J. Dupont, *Angew. Chem. Int. Ed.*, 2014, **53**, 12817-12821.
43. H. E. Gottlieb, V. Kotlyar and A. Nudelman, *J. Org. Chem.*, 1997, **62**, 7512-7515.
44. M. C. Corvo, J. Sardinha, S. C. Menezes, S. Einloft, M. Seferin, J. Dupont, T. Casimiro and E. J. Cabrita, *Angew. Chem. Int. Ed.*, 2013, **52**, 13024-13027.
45. M. C. Corvo, J. Sardinha, T. Casimiro, G. Marin, M. Seferin, S. Einloft, S. C. Menezes, J. Dupont and E. J. Cabrita, *ChemSusChem*, 2015, **8**, 1935-1946.
46. J. D. Holbrey, W. M. Reichert, M. Nieuwenhuyzen, O. Sheppard, C. Hardacre and R. D. Rogers, *Chem. Commun.*, 2003, 476-477.
47. B. C. Leal, J. D. Scholten, M. C. Alves, J. Morais, I. de Pedro, L. Fernandez Barquin and J. Dupont, *Inorg. Chem.*, 2016, **55**, 865-870.
48. P. Lozano, T. de Diego, D. Carrie, M. Vaultier and J. L. Iborra, *Chem. Commun.*, 2002, 692.
49. R. Giernoth and D. Bankmann, *Eur. J. Org. Chem.*, 2008, DOI: 10.1002/ejoc.200700784, 2881-2886.
50. A. Furstner, M. Alcarazo, R. Goddard and C. W. Lehmann, *Angew. Chem. Int. Ed.*, 2008, **47**, 3210-3214.
51. V. Farmer and T. Welton, *Green Chem.*, 2002, **4**, 97-102.
52. X. Chen, X. Li, H. Song, Y. Qian and F. Wang, *Tetrahedron Lett.*, 2011, **52**, 3588-3591.
53. O. V. Dolomanov, L. J. Bourhis, R. J. Gildea, J. A. K. Howard and H. Puschmann, *J. Appl. Crystallogr.*, 2009, **42**, 339-341.
54. R. J. Gildea, L. J. Bourhis, O. V. Dolomanov, R. W. Grosse-Kunstleve, H. Puschmann, P. D. Adams and J. A. K. Howard, *J. Appl. Crystallogr.*, 2011, **44**, 1259-1263.
55. G. M. Sheldrick, *Acta Crystallogr. Sect. A*, 2008, **64**, 112-122.
56. J. D. Chai and M. Head-Gordon, *Phys. Chem. Chem. Phys.*, 2008, **10**, 6615-6620.
57. R. A. Kendall, T. H. Dunning and R. J. Harrison, *J. Chem. Phys.*, 1992, **96**, 6796-6806.
58. G. W. T. M. J. Frisch, H. B. Schlegel, G. E. Scuseria, M. A. Robb, J. R. Cheeseman, G. Scalmani, V. Barone, B. Mennucci, G. A. Petersson, H. Nakatsuji, M. Caricato, X. Li, H. P. Hratchian,A. F. Izmaylov, J. Bloino, G. Zheng, J. L. Sonnenberg, M. Hada, M. Ehara, K. Toyota, R. Fukuda, J. Hasegawa, M. Ishida, T. Nakajima, Y. Honda, O. Kitao, H. Nakai, T. Vreven, J. A. Montgomery, Jr., J. E. Peralta, F. Ogliaro, M. Bearpark, J. J. Heyd, E. Brothers, K. N. Kudin, V. N. Staroverov, T. Keith, R. Kobayashi, J. Normand, K. Raghavachari, A. Rendell, J. C. Burant, S. S. Iyengar, J. Tomasi, M. Cossi, N. Rega, J. M. Millam, M. Klene, J. E. Knox, J. B. Cross, V. Bakken, C. Adamo, J. Jaramillo, R. Gomperts, R. E. Stratmann, O. Yazyev, A. J. Austin, R. Cammi, C. Pomelli, J. W. Ochterski, R. L. Martin, K. Morokuma, V. G. Zakrzewski, G. A. Voth, P. Salvador, J. J. Dannenberg, S. Dapprich, A. D. Daniels, O. Farkas, J. B. Foresman, J. V. Ortiz, J. Cioslowski, and D. J. Fox, *Journal*, 2013.
59. J. de Andrade, E. S. Boes and H. Stassen, *J. Phys. Chem. B*, 2002, **106**, 13344-13351.
60. B. Hess, C. Kutzner, D. van der Spoel and E. Lindahl, *J. Chem. Theory Comput.*, 2008, **4**, 435-447.
61. G. Bussi, D. Donadio and M. Parrinello, *J. Chem. Phys.*, 2007, **126**, AN:014101.
62. M. Parrinello and A. Rahman, *J. Appl. Phys.*, 1981, **52**, 7182-7190.
63. B. Hess, H. Bekker, H. J. C. Berendsen and J. Fraaije, *J. Comput. Chem.*, 1997, **18**, 1463-1472.
64. S. Miyamoto and P. A. Kollman, *J. Comput. Chem.*, 1992, **13**, 952-962.
65. U. Essmann, L. Perera, M. L. Berkowitz, T. Darden, H. Lee and L. G. Pedersen, *J. Chem. Phys.*, 1995, **103**, 8577-8593.
66. C. Caleman, P. J. van Maaren, M. Y. Hong, J. S. Hub, L. T. Costa and D. van der Spoel, *J. Chem. Theory Comput.*, 2012, **8**, 61-74.
67. J. M. Wang, R. M. Wolf, J. W. Caldwell, P. A. Kollman and D. A. Case, *J. Comput. Chem.*, 2004, **25**, 1157-1174.
68. W. L. Jorgensen, J. Chandrasekhar, J. D. Madura, R. W. Impey and M. L. Klein, *J. Chem. Phys.*, 1983, **79**, 926-935.

1